Ca^{2+} sparks activate K^+ and Cl^- channels, resulting in spontaneous transient currents in guinea-pig tracheal myocytes

Ronghua ZhuGe*†, Stephen M. Sims‡, Richard A. Tuft*†, Kevin E. Fogarty*† and John V. Walsh Jr*

**Department of Physiology and †Biomedical Imaging Group, University of Massachusetts Medical School, Worcester, MA 01655, USA and ‡Department of Physiology, University of Western Ontario, London, Ontario, Canada, N6A 5C1*

(Received 13 July 1998; accepted after revision 30 September 1998)

1. Local changes in cytosolic [Ca^{2+}] were imaged with a wide-field, high-speed, digital imaging system while membrane currents were simultaneously recorded using whole-cell, perforated patch recording in freshly dissociated guinea-pig tracheal myocytes.

2. Depending on membrane potential, Ca^{2+} sparks triggered 'spontaneous' transient inward currents (STICs), 'spontaneous' transient outward currents (STOCs) and biphasic currents in which the outward phase always preceded the inward (STOICs). The outward currents resulted from the opening of large-conductance Ca^{2+}-activated K^+ (BK) channels and the inward currents from Ca^{2+}-activated Cl^- (Cl_{Ca}) channels.

3. A single Ca^{2+} spark elicited both phases of a STOIC, and sparks originating from the same site triggered STOCs, STICs and STOICs, depending on membrane potential.

4. STOCs had a shorter time to peak (TTP) than Ca^{2+} sparks and a much shorter half-time of decay. In contrast, STICs had a somewhat longer TTP than sparks but the same half-time of decay. Thus, the STIC, not the STOC, more closely reflected the time course of cytosolic Ca^{2+} elevation during a Ca^{2+} spark.

5. These findings suggest that Cl_{Ca} channels and BK channels may be organized spatially in quite different ways in relation to points of Ca^{2+} release from intracellular Ca^{2+} stores. The results also suggest that Ca^{2+} sparks may have functions in smooth muscle not previously suggested, such as a stabilizing effect on membrane potential and hence on the contractile state of the cell, or as activators of voltage-gated Ca^{2+} channels due to depolarization mediated by STICs.

Calcium ions serve as an intracellular signal for a great variety of processes in one and the same cell. Therefore, the spatial organization of Ca^{2+} signalling in subcellular domains or 'microdomains' has become the focus of many studies (Berridge, 1997). Transient, localized elevations in cytosolic [Ca^{2+}] ($[Ca^{2+}]_i$) have been observed in preparations as diverse as *Xenopus* oocytes (Ca^{2+} 'puffs') (Parker & Yao, 1991) and vertebrate myocytes (Ca^{2+} 'sparks') (Cheng *et al.* 1993; Tsugorka *et al.* 1995). Smooth muscle cells are of special interest in this regard, because Ca^{2+} sparks exert a clear influence on the smooth muscle surface membrane by activating large-conductance Ca^{2+}-activated K^+ channels (BK channels), resulting in spontaneous transient outward currents (STOCs). It is now well established that release of Ca^{2+} from intracellular stores, and not Ca^{2+} influx from the cell exterior, is the proximate cause of STOCs in smooth muscle cells (for review, see Bolton & Imaizumi, 1996). This is also true of neurons where such spontaneous transient outward currents were first observed and designated as spontaneous miniature outward currents or SMOCs (Brown *et al.* 1983). More recently the causal relationship between Ca^{2+} sparks and STOCs has been established, and their physiological role in smooth muscle has been explored by others and ourselves (Nelson *et al.* 1995; Mironneau *et al.* 1996; Kirber *et al.* 1996; ZhuGe *et al.* 1998).

In addition to STOCs, many types of smooth muscle also display spontaneous transient inward currents (STICs), caused by Ca^{2+}-activated Cl^- channels (Cl_{Ca} channels) and first observed in myocytes from trachea (Janssen & Sims, 1992) and portal vein (Wang *et al.* 1992; for review, see Large & Wang, 1996). However, the underlying elevations in $[Ca^{2+}]_i$ that cause the STICs have not been observed previously, leaving a number of questions unanswered. First, are STICs caused by Ca^{2+} sparks, i.e. localized, transient

elevations in $[Ca^{2+}]_i$? If so, do Ca^{2+} sparks arising from the same site trigger both STOCs and STICs? Finally, in cells generating both STICs and STOCs, does the STOC reflect the time course of the underlying Ca^{2+} spark, as one study has suggested (Hogg *et al.* 1993); or does the longer lasting STIC more closely reflect the time course of the Ca^{2+} spark, as others have proposed (Henmi *et al.* 1996)? This last question has generated some controversy, and the answer may have implications for the localization of BK and Cl_{Ca} channels in relation to the Ca^{2+} release sites (see Discussion).

Here we employ freshly dissociated smooth muscle cells from guinea-pig trachea to study STICs and the elevations in $[Ca^{2+}]_i$ that cause them. We chose these cells because their STICs are representative of STICs in many smooth muscle cell types (Large & Wang, 1996) and because they are well characterized. Of special consequence for the present study, STICs in this preparation are known to be caused by Cl_{Ca} channels, and the activating Ca^{2+} comes from intracellular stores, that is from the sarcoplasmic reticulum (SR) (Janssen & Sims, 1992; Henmi *et al.* 1995, 1996). Furthermore, the STOCs observed in this preparation are elicited by Ca^{2+} released into the cytosol from an intracellular source and they are caused by BK channel activation. In these and other respects the STOCs in this preparation are typical of those found in many smooth muscle cell types (Henmi *et al.* 1996; Bolton & Imaizumi, 1996).

In the present study, by simultaneously recording membrane currents and imaging $[Ca^{2+}]_i$ at high temporal resolution with a unique digital imaging system, we demonstrate for the first time the existence of Ca^{2+} sparks that cause STICs. We show that, within the limits of our resolution, Ca^{2+} sparks from the same site can elicit both STICs and STOCs as well as biphasic miniature currents. We designate such biphasic currents as STOICs (i.e. STOC followed by STIC), because the outward phase precedes the inward phase in all cases. Moreover, the decay of the STICs, not STOCs, parallels the decay in $[Ca^{2+}]$ during a Ca^{2+} spark. Based on these data, we suggest that BK and Cl_{Ca} channels may have different spatial relationships to the SR Ca^{2+} release sites. Finally, we suggest possible new roles for Ca^{2+} sparks, either as stabilizers of membrane potential and hence of the contractile state of the cells, or as activators of voltage-activated Ca^{2+} channels via membrane depolarization mediated by Cl_{Ca} channels.

METHODS

Single smooth muscle cells were enzymatically dispersed from the guinea-pig trachea as described previously (Janssen & Sims, 1992). Animals (250–300 g) were anaesthetized with intraperitoneally injected pentobarbital (pentobarbitone; 150 mg kg^{-1}) and then exsanguinated under deep anaesthesia following which tissue collection was carried out. All animal care and tissue collections were performed in accordance with the guidelines of the Animal Care Committee of the University of Massachusetts Medical School. Membrane currents were recorded with an Axopatch-1D amplifier (Axon Instruments) using the perforated patch configuration. Extracellular solution contained (mM): 130 NaCl, 3 KCl, 1·8 $CaCl_2$, 1 $MgCl_2$, 10 Hepes; pH adjusted to 7·4 with NaOH. Pipette solution contained (mM): 137 KCl, 3 $MgCl_2$, 10 Hepes and amphotericin B (200 μg ml^{-1}); pH adjusted to 7·2 with KOH. All experiments were carried out at room temperature (20–23 °C). Recordings of whole-cell currents were low-pass filtered (200 Hz cut-off), digitally sampled at 1 kHz and stored for analysis.

Fluorescence images of cytosolic free Ca^{2+} using fluo-3 as a calcium indicator (loaded by 30 min incubation with 10 μM fluo-3 AM) was achieved using a custom-built wide-field digital imaging system. The system can acquire images at a maximum speed of 550 Hz, thus providing a temporal resolution comparable to the confocal line-scan technique but with a much larger observed area. Such rapid imaging was made possible by using a cooled high-sensitivity, charge-coupled device camera developed in conjunction with MIT Lincoln Laboratories (Lexington, MA, USA). For these experiments a circular image-buffer system was employed to facilitate the capture of spontaneous events, and for this arrangement, image exposure time was either 7 or 10 ms, with a 7 ms inter-image wait, yielding a cycle time of either 14 or 17 ms. The camera was interfaced to a custom-made inverted microscope. The 488 nm line of a multiline Argon laser provided fluorescence excitation, and a laser shutter controlled the exposure duration. Emission of the Ca^{2+} indicator was monitored at wavelengths greater than 500 nm. Subsequent image processing and analysis were performed off-line using a custom-designed software package, running on a Silicon Graphics workstation. Ca^{2+} images were derived on a pixel to pixel basis from the equation:

$$\Delta F/F_0(\%) = 100 \times [F(x,y,t) - F_0(x,y)]/F_0(x,y),$$

where $F(x,y,t)$ is the fluorescence at each pixel in the time series and F_0 is an image of the 'resting' level derived from the fluorescence time series by computing the mean pixel value during quiescent times at each $F(x,y)$. The change in fluorescence provides only a relative, not an absolute, measurement of free Ca^{2+} concentration. (Extensive ratiometric measurements of resting $[Ca^{2+}]_i$ with fura-2 have previously been carried out on the cells used here, isolated in the same way and under the same conditions of recording; the resting $[Ca^{2+}]_i$ was found to be 105 ± 10 nM (mean ± S.E.M.) (Sims *et al.* 1996).) An increase in fluorescence was considered to be a Ca^{2+} spark when it was equal to or greater than 5·0% and lasted for at least two frames.

Fluo-3 AM was purchased from Molecular Probes and all other chemicals from Sigma.

RESULTS

We employed ultra-fast, wide-field digital imaging and perforated patch recording to monitor simultaneously Ca^{2+} sparks and membrane currents in a total of 62 freshly dissociated tracheal smooth muscle cells from guinea-pigs. (Ca^{2+} sparks were observed in an additional 60 cells which were not concurrently patched.) E_{Cl} in all recordings was approximately 0 mV and E_K was −96 mV. At sufficiently negative potentials (generally −50 mV or more negative), Ca^{2+}sparks were associated with synchronous STICs (Fig. 1). Furthermore, the time course of the decay of the STIC paralleled that of the spark. The STICs, but not the Ca^{2+} sparks, were reversibly blocked by 100 μM niflumic acid (data not shown), a blocker of Cl_{Ca} channels (Janssen & Sims, 1992; Hogg *et al.* 1994; Henmi *et al.* 1995, 1996),

providing further evidence that these sparks triggered the STICs. Moreover, as illustrated in Fig. 1, Ca^{2+} sparks were readily recorded at potentials below −90 mV, suggesting that Ca^{2+} entry through voltage-activated Ca^{2+} channels is not necessary to elicit them. Finally, in six unpatched cells, ryanodine (100 μM) abolished Ca^{2+} sparks (data not shown), indicating that they arise from opening of ryanodine receptors and not from Ca^{2+} entry from the exterior. Thus, Ca^{2+} sparks, due to release of Ca^{2+} from internal stores via ryanodine receptors, trigger STICs.

It has previously been shown in these and other smooth muscle cells that, at potentials between E_K and E_{Cl}, spontaneous biphasic currents occur and that BK channels and Cl_{Ca} channels underlie their outward and inward phases, respectively (Wang *et al.* 1992; Janssen & Sims, 1994; Henmi *et al.* 1995). Are such biphasic currents triggered by a single spark? We found that at such intermediate potentials, a single Ca^{2+} spark was accompanied by a biphasic current for which the outward phase preceded the inward in every instance (Fig. 2), and hence these biphasic currents are designated as STOICs (i.e. STOC followed by STIC). Consistent with earlier studies, we found that the inward phase of the STOICs elicited by Ca^{2+} sparks was reversibly blocked by niflumic acid (100 μM; data not shown). Moreover, as can be seen in Fig. 2, the decay of the inward phase of

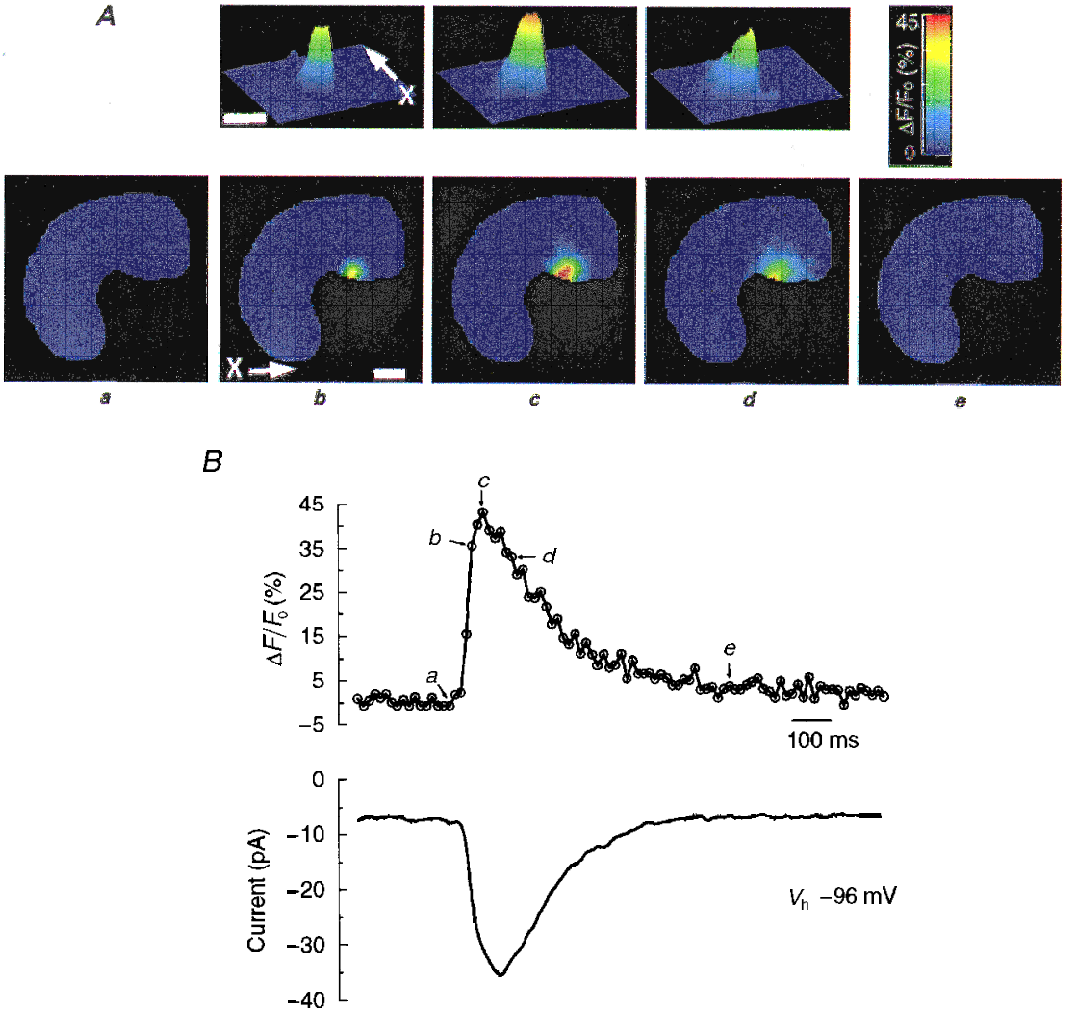

Figure 1. A single Ca^{2+} spark and the resulting STIC, recorded simultaneously at high temporal resolution

A, images showing the time course of a single Ca^{2+} spark acquired at the times designated in the upper trace of *B*. Images in the lower row of *A* show the entire cell. Contour plots in the upper row of *A* show the spark at higher spatial resolution. The arrow and 'X' in the contour plot mark the axis corresponding to the *x*-axis in the 2-D image below. The same convention is employed in subsequent figures. Each point is the result of a 10 ms exposure. Calibration bar is 5 μm. *B*, upper trace tracks the time course of the change in $[Ca^{2+}]$ in the one pixel (333 nm × 333 nm) where the peak $[Ca^{2+}]$ is reached during the course of the spark. Lower trace shows the inward current simultaneously recorded at a holding potential (V_h) of −96 mV, employing perforated patch recording as described in Methods.

current, but not that of the outward phase, paralleled the decay of the Ca^{2+} spark.

Since the same spark can activate both BK and Cl_{Ca} channels during the course of a STOIC, it seemed that sparks arising from the same site should be able to activate a STIC or STOC, depending on the membrane potential. Within the limits of our resolution this was indeed the case. At 0 mV, E_{Cl} in these experiments, Ca^{2+} sparks were accompanied by outward currents or STOCs (Fig. 3, column *a*) which are caused by BK channels in these cells and many others (Henmi *et al.* 1995; Bolton & Imaizumi, 1996). As shown in Fig. 3, Ca^{2+} sparks arising from the same site generated STOCs, STICs or STOICs, depending on membrane potential. In the case of the STOC, the outward current returned to rest while the local cytosolic $[Ca^{2+}]$ due to the spark was still elevated. The time course of a series of Ca^{2+} sparks and the STICs which they elicited at −60 mV were compared. The mean ± S.E.M. time to peak (TTP) of these sparks was 92 ± 8 ms ($n = 17$) which was shorter than the 130 ± 17 ms for the STICs ($P < 0{\cdot}02$, Student's paired t test). The half-time of decay was not significantly different for these sparks and STICs: 150 ± 16 and 182 ± 21 ms, respectively. The time courses of a series of Ca^{2+} sparks and the STOCs which they elicited at 0 mV were also compared. In this series the TTP was 55 ± 4 ms for the Ca^{2+} sparks, which was significantly longer than the 30 ± 2 ms for the STOCs ($P < 10^{-7}$, $n = 26$). (Correcting for differences in onsets, the peak of the STOC preceded that of the spark by 16 ± 3 ms.) The half-time of decay was 135 ± 16 ms for these sparks, which was significantly longer than the

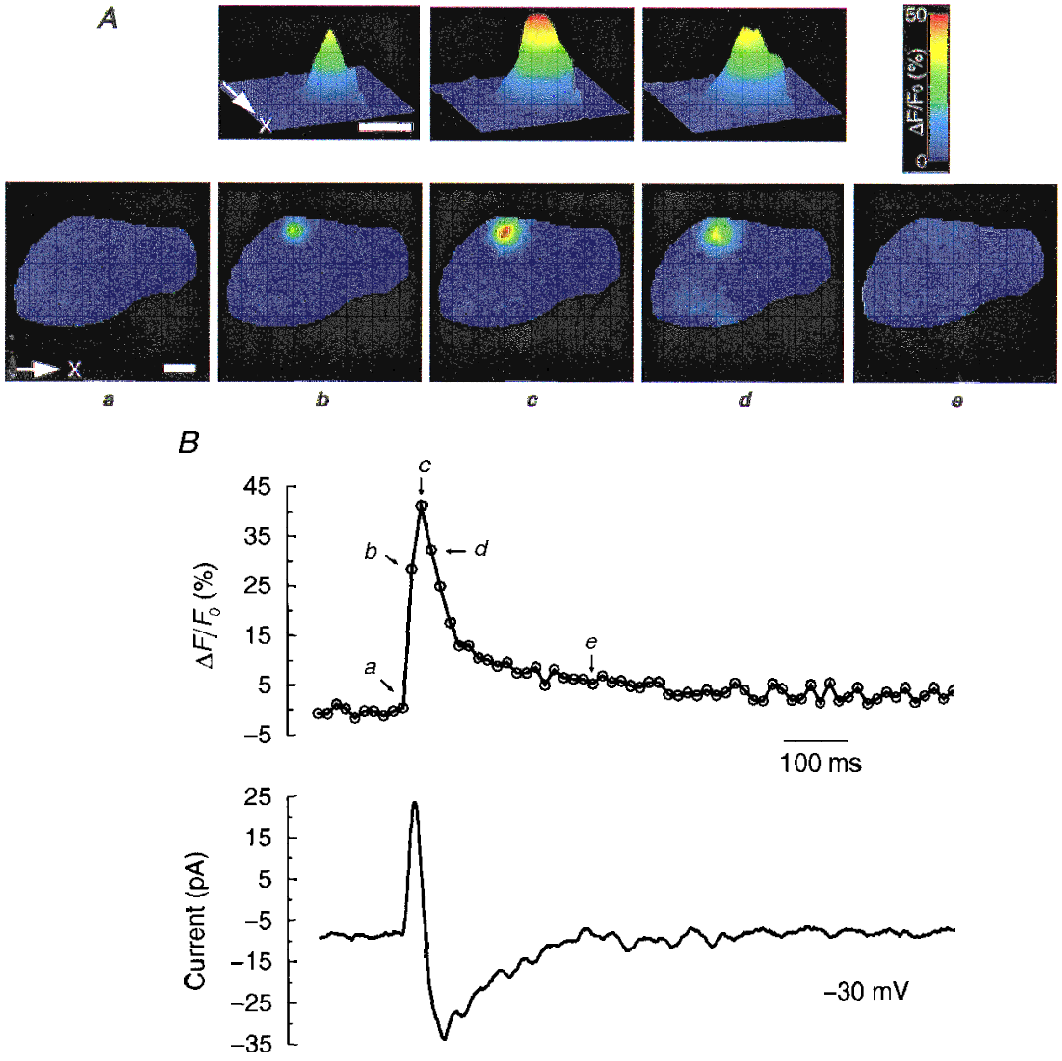

Figure 2. A single Ca^{2+} spark and the resulting biphasic current (STOIC)

A, images showing the time course of a single Ca^{2+} spark acquired at the times designated in the upper trace of *B*. Images in the lower row of *A* show the entire cell. Contour plots in the upper row of *A* show the spark at higher spatial resolution. Calibration bar is 5 μm. *B*, upper trace tracks the time course of the change in $[Ca^{2+}]$ in the one pixel (333 nm × 333 nm) where the peak $[Ca^{2+}]$ is reached during the course of the spark. Lower trace shows the current simultaneously recorded at a holding potential of −30 mV.

43 ± 5 ms for the STOCs ($P < 10^{-5}$). In summary, the time course of the STOCs did not parallel that of the Ca^{2+} sparks; the STOCs reached their peak faster than the Ca^{2+} sparks, and they decayed several times faster. In contrast, although the STICs rose somewhat more slowly than the Ca^{2+} sparks, their half-times of decay were not different. Hence, the time course of the STICs rather than the STOCS more closely paralleled that of the Ca^{2+} sparks.

The wide-field, high-speed digital imaging system made it readily possible to construct maps, in a single cell, of the Ca^{2+} spark sites that give rise to transient currents. Such a map is shown in Fig. 4*A*, where each circle indicates the location and amplitude (the latter proportional to the radius of the circle) of one Ca^{2+} spark which triggers a biphasic current, i.e. a STOIC. The map shows that Ca^{2+} sparks which are able to trigger both outward and inward phases of a miniature current (and hence both STICs and STOCs) are not restricted to one region of the cell. Moreover, it also appeared from maps like these that some sites discharged at a considerably higher frequency than others (See Kirber *et al.* 1996; ZhuGe *et al.* 1998; Gordienko *et al.* 1998).

If the same spark is responsible for both inward and outward phases of current, then one might expect the amplitude of both phases to correlate with the amplitude of the corresponding Ca^{2+} spark. Figure 4*B* is a plot of the peak amplitude of each of the Ca^{2+} sparks from the same cell mapped in Fig. 4*A* against the amplitude of both the inward and outward phases of the STOIC caused by that spark. The amplitude of both the inward and outward phases of current were correlated with the amplitude of the corresponding spark. However, the correlation was weak in each case. (For the example shown in Fig. 4*B*, the correlation coefficient was

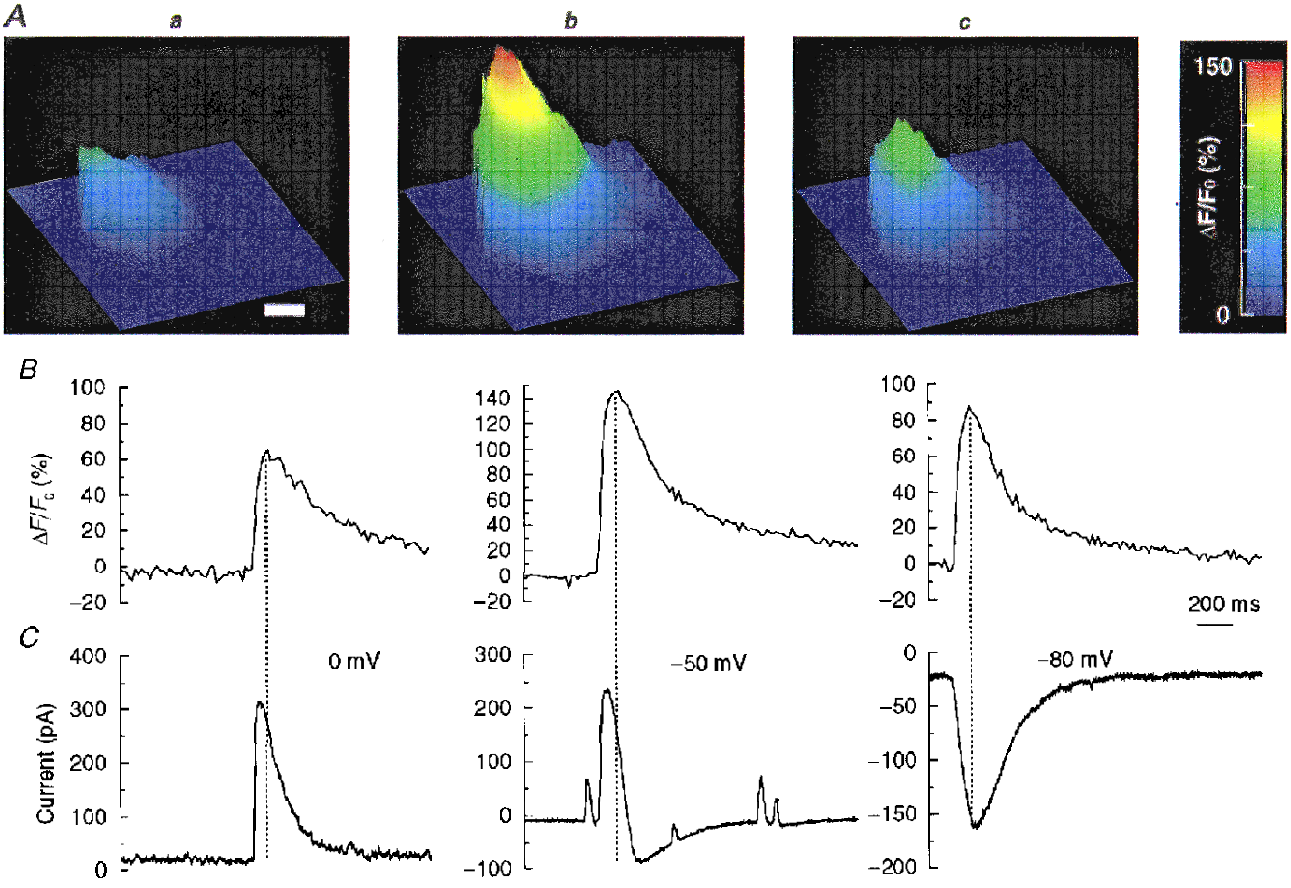

Figure 3. Time course of Ca^{2+} sparks and corresponding currents

Three Ca^{2+} sparks arising from the same site cause a STOC, STIC or STOIC, depending on membrane potential. Each column (*a–c*) represents three different sparks, all occurring at the same site, and the membrane current recorded simultaneously. Note that sparks occurring at the same site can vary in amplitude. *A*, contour plot constructed from image (10 ms exposure) acquired at the peak of each of the three Ca^{2+} sparks. The contour plots are flattened on the left, because that is the location of the cell membrane. Calibration bar is 5 μm. *B*, the time course of the [Ca^{2+}] change for the pixel (333 nm × 333 nm) where the peak [Ca^{2+}] occurred during each spark. *C*, currents recorded simultaneously at the three different holding potentials indicated; from left to right, a STOC, STOIC and STIC.

0·52 for the outward phase and 0·63 for the inward phase.) This finding is consistent with one and the same Ca^{2+} spark acting to cause both phases of current. The plot also makes evident the considerable variation in the size of sparks and the currents which they elicit.

DISCUSSION

In the present study we have imaged Ca^{2+} sparks which cause STICs, STOCs and STOICs. The same Ca^{2+} sparks are capable of eliciting both the outward phase and subsequent inward phase of current found in STOICs, which are caused, respectively, by BK and Cl_{Ca} channels. Within the limits of our resolution, the same spark site can cause a STIC, a STOC or a STOIC depending on membrane potential. This study has implications both for the physiological role of Ca^{2+} sparks and for the organization of the BK and Cl_{Ca} channels with respect to a Ca^{2+} release site.

Physiological roles of Ca^{2+} sparks in smooth muscle

In certain smooth muscle types, for example, those from rat cerebral arteries, Ca^{2+} sparks elicit only STOCs; and for such cells Nelson *et al.* (1995) have provided evidence that Ca^{2+} sparks lead to hyperpolarization and hence to relaxation of smooth muscle. One appeal of their proposal is that it provides a specific physiological role for sparks themselves. However, such a hypothesis encounters a difficulty if applied to those smooth muscle cell types where Ca^{2+} sparks elicit not only STOCs, but also STICs, which will depolarize a cell when it is at rest. (In smooth muscle E_{Cl} is generally found to lie between −30 and −20 mV, and the resting potential to lie between −50 and −75 mV (Large & Wang, 1996; Nelson *et al.* 1997).) Moreover, Cl^- channels are now recognized as key determinants of membrane potential in many smooth muscle cells, contributing to depolarization and contraction (Large & Wang, 1996; Hashitani *et al.* 1996; Nelson *et al.* 1997; Yuan, 1997). A partial resolution of this difficulty is to postulate that STOCs and STICs are elicited by different SR Ca^{2+} release sites, but the results of the present study argue against this. We suggest that Ca^{2+} sparks have functions other than causing relaxation. Two possibilities suggest themselves.

First, Ca^{2+} sparks may exert a negative feedback or stabilizing influence on membrane potential. Thus, inward Cl^- current will be the dominant current elicited when a Ca^{2+} spark occurs at more negative potentials, closer to E_K and farther from E_{Cl}; and outward K^+ current will dominate at less negative potentials. Moreover, if the resting level of membrane potential determines the contractile state by turning Ca^{2+} 'window' currents on or off as Nelson *et al.* (1995) have proposed, then the stabilizing effect of sparks on membrane potential will translate into a stabilizing effect on the cell's contractile state. Thus, sparks may serve to stabilize the membrane potential and perhaps also the contractile state of those smooth muscle cells which have both STICs and STOCs. A second and quite different function is suggested by the order of the biphasic currents (STOICs), which is always outward then inward at potentials near apparent rest. Under current clamp in many cells STOICs translate into a brief hyperpolarization followed by a depolarization (see Janssen & Sims, 1992, Fig. 8a). Such biphasic potentials, properly synchronized, might lead to activation of voltage-activated Ca^{2+} channels by an anode-break mechanism and thus elicit contraction (Walsh & Singer, 1980). Finally, Ca^{2+} sparks might serve both of these

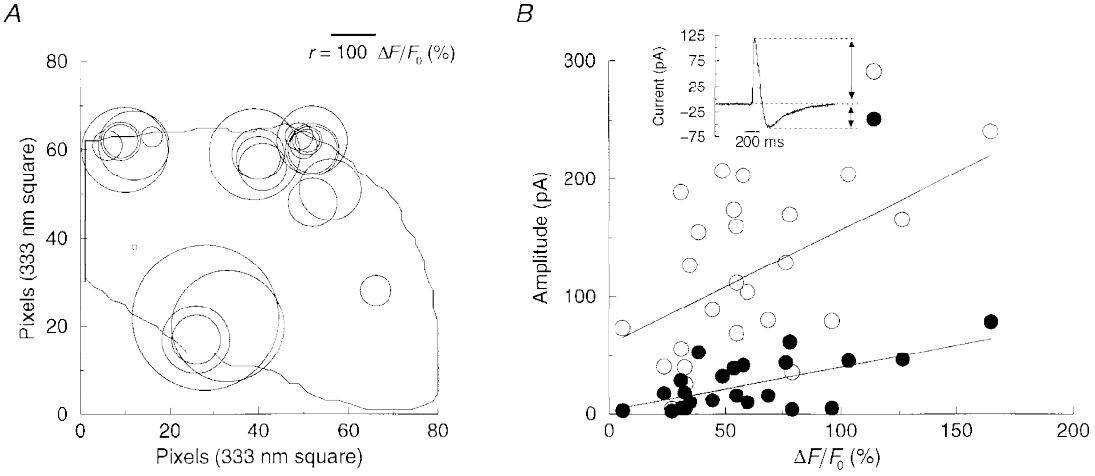

Figure 4. Distribution of Ca^{2+} sparks and characteristics of corresponding biphasic currents in a tracheal muscle cell

A, 'spark map' for one cell showing the location of all sparks that gave rise to STOICs over an observation period of 18 s at a holding potential of −50 mV. Centre of each circle corresponds to the peak of one spark and the radius, *r*, is equal to the peak amplitude ($\Delta F/F_0$ (%)) of the spark, as shown by the scale bar. *B*, plot of spark amplitude *versus* the outward (○) and inward (●) component of the STOIC caused by each spark. Plot is for same set of sparks in map of *A*, and hence all data points are from the same cell. Inset shows a STOIC.

functions, depending on the membrane potential and the state of the BK and Cl_{Ca} channels, both of which are capable of substantial modulation.

The organization of BK channels and Cl_{Ca} channels within the Ca^{2+} spark microdomain

The precise relationship of the time course of the Ca^{2+} sparks to those of the STOCs, STICs and STOICs has implications for the spatial organization of BK and Cl_{Ca} channels in relation to the ryanodine receptors at the spark site. A STOC in these cells characteristically decayed faster than the Ca^{2+} spark causing it, whereas a STIC decayed in parallel with the eliciting spark. The simplest interpretation to be drawn from these observations is that the Cl_{Ca} channels are sufficiently sensitive to cytosolic Ca^{2+} to be activated at the low levels of Ca^{2+} concentration during the declining phase of the spark (Pacaud *et al.* 1992; Carl *et al.* 1996). A similar conclusion has been drawn by Henmi *et al.* (1996) from elegant experiments on caffeine-elicited, whole-cell, macroscopic, biphasic currents. In those experiments, during refilling of the SR with Ca^{2+} after transient depletion, the Cl_{Ca} channel current recovered more quickly than did the BK channel current upon caffeine application, leading to the conclusion that the BK channels are less sensitive to Ca^{2+} than the Cl_{Ca} channels.

If, however, the Cl_{Ca} channels are more sensitive to Ca^{2+} than are the BK channels, how are we to explain the fact that, in the case of the biphasic currents (STOICs), the outward phase of current, mediated by BK channels, precedes the inward phase, mediated by Cl_{Ca} channels? This was always the case in the present study, as it was in earlier studies on STICs (Wang *et al.* 1992; Janssen & Sims, 1992; Henmi *et al.* 1996). This apparent contradiction can be resolved, however, by a model in which the BK channels lie very close to a SR Ca^{2+} release site, perhaps within a distance of the order of 100 nm. The BK channels will then be exposed at once to a very high $[Ca^{2+}]$ at the onset of a Ca^{2+} spark and be activated quickly, despite their low sensitivity. In contrast, the ensemble of Cl_{Ca} channels, if not concentrated exclusively at the SR Ca^{2+} release site, will be activated more slowly; and, because of their relatively high sensitivity to Ca^{2+}, they will remain active even as the $[Ca^{2+}]_i$ decays to lower levels. This interpretation is also consistent with the fact that the TTP of the STIC is somewhat longer than that of $[Ca^{2+}]$ at the centre of the initiating spark. This delay presumably reflects the time required for Ca^{2+} ions to reach the more remotely located Cl_{Ca} channels. Thus, the STICs (and the inward phase of the STOICs) will reflect the time course of the change in $[Ca^{2+}]$ over the entire microscopic domain of the Ca^{2+} spark. In contrast, BK channel activity during a Ca^{2+} spark will reflect the $[Ca^{2+}]$ in close proximity to the Ca^{2+} release site.

We note that the STOC begins to decay while the spark is still rising. (That is, the STOC peaks *before* the spark.) Thus, it is possible that the BK channels turn off before the spark is over, not because of diffusion of Ca^{2+} away from the release site, but because they are exposed to Ca^{2+} concentrations high enough to drive them into an inactive state. Inactivation by micromolar cytosolic Ca^{2+} concentrations has been reported recently for BK channels (Rothberg *et al.* 1996; Hicks & Marrion, 1998), including BK channels in smooth muscle cells (Muñoz *et al.* 1998). (Alternatively, a BK channel may be coupled so closely to one ryanodine receptor that overall $[Ca^{2+}]$ may continue to rise in the centre of the spark microdomain even as some ryanodine receptors within it and their associated BK channels are shutting off. This mechanism shares with the inactivation mechanism the requirement that the BK channels be localized very close to the ryanodine receptors at the Ca^{2+} release site.)

Finally, in previous studies on portal vein, where sparks were not monitored, it was argued that the decay of STICs was due principally to slow closure of the Cl_{Ca} channels (i.e. long open times), following a comparatively brief Ca^{2+} transient that was thought to be mirrored by the time course of the STOC (Hogg *et al.* 1993; Large & Wang, 1996). Since the decays of the spark and the STIC paralleled one another in the present study, the precise contribution of the Cl_{Ca} channel kinetics to STIC decay seems uncertain and deserves to be revisited.

In summary, we have demonstrated for the first time that Ca^{2+} sparks activate Cl_{Ca} channels and thus cause STICs. This finding suggests new roles for Ca^{2+} sparks in the regulation of smooth muscle. Moreover, the findings of the present study suggest that BK and Cl_{Ca} channels may be organized spatially in relation to the SR Ca^{2+} release site in radically different ways.

Berridge, M. J. (1997). Elementary and global aspects of calcium signalling. *Journal of Physiology* **499**, 291–306.

Bolton, T. B. & Imaizumi, Y. (1996). Spontaneous transient outward currents in smooth muscle cells. *Cell Calcium* **20**, 141–152.

Brown, D. A., Constanti, A. & Adams, P. R. (1983). Ca-activated potassium current in vertebrate sympathetic neurones. *Cell Calcium* **4**, 407–420.

Carl, A., Lee, H. K. & Sanders, K. M. (1996). Regulation of ion channels in smooth muscles by calcium. *American Journal of Physiology* **271**, C9–34.

Cheng, H., Lederer, W. J. & Cannell, M. B. (1993). Calcium sparks: elementary events underlying excitation-contraction coupling in heart muscle. *Science* **262**, 740–744.

Gordienko, D. V., Bolton, T. B. & Cannell, M. B. (1998). Variability in spontaneous subcellular calcium release in guinea-pig ileum smooth muscle cells. *Journal of Physiology* **507**, 707–720.

Hashitani, H., Van Helden, D. F. & Suzuki, H. (1996). Properties of spontaneous depolarization in circular smooth muscle cells of rabbit urethra. *British Journal of Pharmacology* **118**, 1627–1632.

Henmi, S., Imaizumi, Y., Muraki, K. & Watanabe, M. (1995). Characteristics of caffeine-induced and spontaneous inward currents and related intracellular Ca^{2+} storage sites in guinea-pig tracheal smooth muscle cells. *European Journal of Pharmacology* **282**, 219–228.

Henmi, S., Imaizumi, Y., Muraki, K. & Watanabe, M. (1996). Time course of Ca^{2+}-dependent K^+ and Cl^- currents in single smooth muscle cells of guinea-pig trachea. *European Journal of Pharmacology* **306**, 227–236.

Hicks, G. A. & Marrion, N. V. (1998). Ca^{2+}-dependent inactivation of large conductance Ca^{2+}-activated K^+ (BK) channels in rat hippocampal neurones produced by pore block from an associated particle. *Journal of Physiology* **508**, 721–734.

Hogg, R. C., Wang, Q. & Large, W. A. (1993). Time course of spontaneous calcium-activated chloride currents in smooth muscle cells from the rabbit portal vein. *Journal of Physiology* **464**, 15–31.

Hogg, R. C., Wang, Q. & Large, W. A. (1994). Action of niflumic acid on evoked and spontaneous calcium-activated chloride and potassium currents in smooth muscle cells from rabbit portal vein. *British Journal of Pharmacology* **112**, 977–984.

Janssen, L. J. & Sims, S. M. (1992). Acetylcholine activates non-selective cation and chloride conductance in canine and guinea-pig tracheal myocytes. *Journal of Physiology* **453**, 197–218.

Janssen, L. J. & Sims, S. M. (1994). Spontaneous transient inward currents and rhythmicity in canine and guinea-pig tracheal smooth muscle cells. *Pflügers Archiv* **427**, 473–480.

Kirber, M. T., Etter, E. F., Singer, J. J., Fay, F. S. & Walsh J. V. Jr (1996). Sparks and STOCs in esophageal smooth muscle cells. *Digestive Diseases and Sciences* **41**, 1893.

Large, W. A. & Wang, Q. (1996). Characteristics and physiological role of the Ca^{2+}-activated Cl^- conductance in smooth muscle. *American Journal of Physiology* **271**, C435–454.

Mironneau, J., Arnaudeau, S., Macrez-Lepretre, N. & Boittin, F. X. (1996). Ca^{2+} sparks and Ca^{2+} waves activate different Ca^{2+}-dependent ion channels in single myocytes from rat portal vein. *Cell Calcium* **20**, 153–160.

Muñoz, A., García, L. & Guerrero-Hernández, A. (1998). In situ characterization of the Ca^{2+} sensitivity of large conductance Ca^{2+}-activated K^+ channels: Implications for their use as near-membrane Ca^{2+} indicators in smooth muscle cells. *Biophysical Journal* **75**, 1774–1782.

Nelson, M. T., Cheng, H., Rubart, M., Santana, L. F., Bonev, A. D., Knot, H. J. & Lederer, W. J. (1995). Relaxation of arterial smooth muscle by calcium sparks. *Science* **270**, 633–637.

Nelson, M. T., Conway, M. A., Knot, H. J. & Brayden, J. E. (1997). Chloride channel blockers inhibit myogenic tone in rat cerebral arteries. *Journal of Physiology* **502**, 259–264.

Pacaud, P., Loirand, G., Gregoire, G., Mironneau, C. & Mironneau, J. (1992). Calcium-dependence of the calcium-activated chloride current in smooth muscle cells of rat portal vein. *Pflügers Archiv* **421**, 125–130.

Parker, I. & Yao, Y. (1991). Regenerative release of calcium from functionally discrete subcellular stores by inositol trisphosphate. *Proceedings of the Royal Society* B **246**, 269–274.

Rothberg, B. S., Bello, R. A., Song, L. & Magleby, K. L. (1996). High Ca^{2+} concentrations induce a low activity mode and reveal Ca^{2+}-independent long shut intervals in BK channels from rat muscle. *Journal of Physiology* **493**, 673–689.

Sims, S. M., Jiao, Y. & Zheng, Z. G. (1996). Intracellular calcium stores in isolated tracheal smooth muscle cells. *American Journal of Physiology* **271**, L300–309.

Tsugorka, A., Ríos, E. & Blatter, L. A. (1995). Imaging elementary events of calcium release in skeletal muscle cells. *Science* **269**, 1723–1726.

Walsh, J. V. Jr & Singer, J. J. (1980). Calcium action potential in single freshly isolated smooth muscle cells. *American Journal of Physiology* **239**, C162–174.

Wang, Q., Hogg, R. C. & Large, W. A. (1992). Properties of spontaneous inward currents recorded in smooth muscle cells isolated from the rabbit portal vein. *Journal of Physiology* **451**, 525–537.

Yuan, X. J. (1997). Role of calcium-activated chloride current in regulating pulmonary vasomotor tone. *American Journal of Physiology* **272**, L959–968.

ZhuGe, R., Tuft, R. A., Fogarty, K. E. & Walsh, J. V. Jr (1998). Microdomains mediating generation of Ca^{2+} sparks and STOCs in smooth muscle cells. *Biophysical Journal* **74**, 272.

Acknowledgements

We thank Rebecca McKinney for excellent technical assistance, and Robert Drummond and Agustine Guerrero-Hernández for their very helpful comments on the manuscript. This study was supported by grants from the National Institutes of Health to J.V.W. and R.A.T. and a grant from the National Science Foundation to R.A.T. S.M.S. was supported by the MRC of Canada.

Corresponding author

J. V. Walsh Jr: Department of Physiology, University of Massachusetts Medical Center, Worcester, MA 01605, USA.

Email: john.walsh@ummed.edu